Mouse MOV10L1 associates with Piwi proteins and is an essential component of the Piwi-interacting RNA (piRNA) pathway

Ke Zheng[a,1], Jordi Xiol[b,1], Michael Reuter[b], Sigrid Eckardt[c], N. Adrian Leu[a], K. John McLaughlin[c], Alexander Stark[d], Ravi Sachidanandam[e], Ramesh S. Pillai[b,2], and Peijing Jeremy Wang[a,2]

[a]Center for Animal Transgenesis and Germ Cell Research and Department of Animal Biology, University of Pennsylvania School of Veterinary Medicine, Philadelphia, PA 19104; [b]European Molecular Biology Laboratory, Grenoble Outstation, 38042 Grenoble, France; [c]Research Institute at Nationwide Children's Hospital, Columbus, OH 43205; [d]Research Institute of Molecular Pathology (IMP), A-1030 Vienna, Austria; and [e]Department of Genetics and Genomic Sciences, Mount Sinai School of Medicine, New York, NY 10029

Edited by Brigid L. M. Hogan, Duke University Medical Center, Durham, NC, and approved May 11, 2010 (received for review March 25, 2010)

Piwi-interacting RNAs (piRNAs) are essential for silencing of transposable elements in the germline, but their biogenesis is poorly understood. Here we demonstrate that MOV10L1, a germ cell–specific putative RNA helicase, is associated with Piwi proteins. Genetic disruption of the MOV10L1 RNA helicase domain in mice renders both MILI and MIWI2 devoid of piRNAs. Absence of a functional piRNA pathway in *Mov10l1* mutant testes causes loss of DNA methylation and subsequent derepression of retrotransposons in germ cells. The *Mov10l1* mutant males are sterile owing to complete meiotic arrest. This mouse mutant expresses Piwi proteins but lacks piRNAs, suggesting that MOV10L1 is required for piRNA biogenesis and/or loading to Piwi proteins.

meiosis | RNA helicase | transposon silencing

The Piwi clade of Argonaute proteins associates with a class of 26–31-nt germline-specific small RNAs called "piRNAs". Together they participate in suppression of transposable elements in all animals studied (1–4). In mice, the Piwi clade contains three members: *Miwi2*, *Mili*, and *Miwi*. These three Piwi members exhibit distinct developmental expression patterns. *Miwi2* is expressed in perinatal male germ cells (5), whereas *Mili* is more broadly expressed from embryonic germ cells to postnatal round spermatids (6). *Miwi* expression begins in pachytene spermatocytes and persists in haploid round spermatids (7). The overlapping temporal expression of *Mili* with *Miwi* and *Miwi2* points to the pivotal role of MILI in the piRNA pathway, as further supported by the fact that MILI is associated with developmental stage–dependent pools of piRNAs: prenatal, prepachytene, and pachytene piRNAs (5, 8, 9).

The mechanisms of piRNA biogenesis are largely unclear (1–4). One feature of piRNAs in all species is their highly clustered genomic origins. Several of these clusters produce piRNAs only from one strand. This leads to a hypothesized primary processing pathway whereby an unknown nuclease cleaves off mature piRNAs from a long single-stranded precursor transcript. On the other hand, some piRNAs in prenatal and prepachytene pools display signatures indicative of a proposed RNA-mediated amplification loop that uses primary piRNAs to generate secondary piRNAs from precursor transcripts (ping-pong mechanism) (10, 11). Apart from the Piwi proteins themselves, factors directly impacting piRNA production are unknown.

We previously identified *Mov10l1* as a gene specifically expressed in mouse germ cells, which encodes a putative RNA helicase of unknown function (12). Whereas the N-terminal half of MOV10L1 is not homologous to any other mouse proteins, its C-terminal RNA helicase domain exhibits low homology (45% amino acid identity) with MOV10. MOV10, the vertebrate homolog of *Drosophila* Armi, is ubiquitously expressed. In mammalian cells, MOV10 is associated with Argonaute proteins in the RNA-induced silencing complex (RISC) and is functionally required for RNA interference (13, 14). Here we demonstrate that MOV10L1 is an essential factor in the piRNA pathway.

Results

MOV10L1 Is Associated with Piwi Proteins. To identify potential interaction partners, we isolated MOV10L1-containing protein complexes from testicular extracts by immunoprecipitation. Mass spectrometry analyses of three specific protein bands in the MOV-10L1 complex revealed that they corresponded to MOV10L1/TDRD1, MILI, and MIWI (Fig. S1). We and others have also found MOV10L1 in immunoprecipitated MILI, MIWI, and MIWI2 complexes by mass spectrometry (15, 16). Consistent with the mass spectrometry data, coimmunoprecipitations followed by Western blot analysis showed abundant association of MOV10L1 with MILI but less with TDRD1 and MIWI (Fig. 1 *A* and *B*). Further coimmunoprecipitation experiments done with cotransfected human 293T cells strongly suggested that MOV10L1 binds to MILI, MIWI, and MIWI2 (Fig. 1*C*), because mammalian somatic cells lack piRNA pathway components.

To determine whether MOV10L1 is associated with piRNAs, we immunoprecipitated MOV10L1, MILI, and MIWI from adult mouse testes and assessed the presence of any associated small RNAs (Fig. 1*D*). As expected, MILI and MIWI were associated with ≈26-nt and ≈30-nt small RNAs, respectively. Consistent with its interaction with Piwi proteins, the MOV10L1 purification revealed the presence of small RNAs in the 26–30-nt size range, with a majority migrating similar to MILI-associated piRNAs (Fig. 1*D*). It is very likely that MOV10L1 is associated with piRNAs indirectly through its interaction with Piwi proteins.

We then performed Solexa deep sequencing of a small RNA library from MOV10L1 complexes isolated from adult testes. A total of ≈2.2 million reads perfectly mapped to the genome and peaked around 26 to 27 nt (Fig. 1*E*), similar to those in small RNA libraries prepared from MILI or its interacting partner, TDRD1 (17). A notable fraction (≈8%) of MOV10L1 reads was 29–32 nt in length, a size similar to MIWI-associated piRNAs (18, 19). The MOV10L1 reads display a strong preference (≈80%) for a uridine at position one (U1-bias). Genome annotation of the MOV10L1

Author contributions: K.Z., J.X., R.S.P., and P.J.W. designed research; K.Z., J.X., M.R., S.E., N.A.L., and K.J.M. performed research; A.S. and R.S. analyzed data; and R.S.P. and P.J.W. wrote the paper.

The authors declare no conflict of interest.

This article is a PNAS Direct Submission.

Data deposition: Solexa deep-sequencing data have been deposited in the Gene Expression Omnibus (GEO) database, www.ncbi.nlm.nih.gov/geo (accession no. GSE21763).

[1]K.Z. and J.X. contributed equally to this work.

[2]To whom correspondence may be addressed. E-mail: pwang@vet.upenn.edu or pillai@embl.fr.

This article contains supporting information online at www.pnas.org/lookup/suppl/doi:10.1073/pnas.1003953107/-/DCSupplemental.

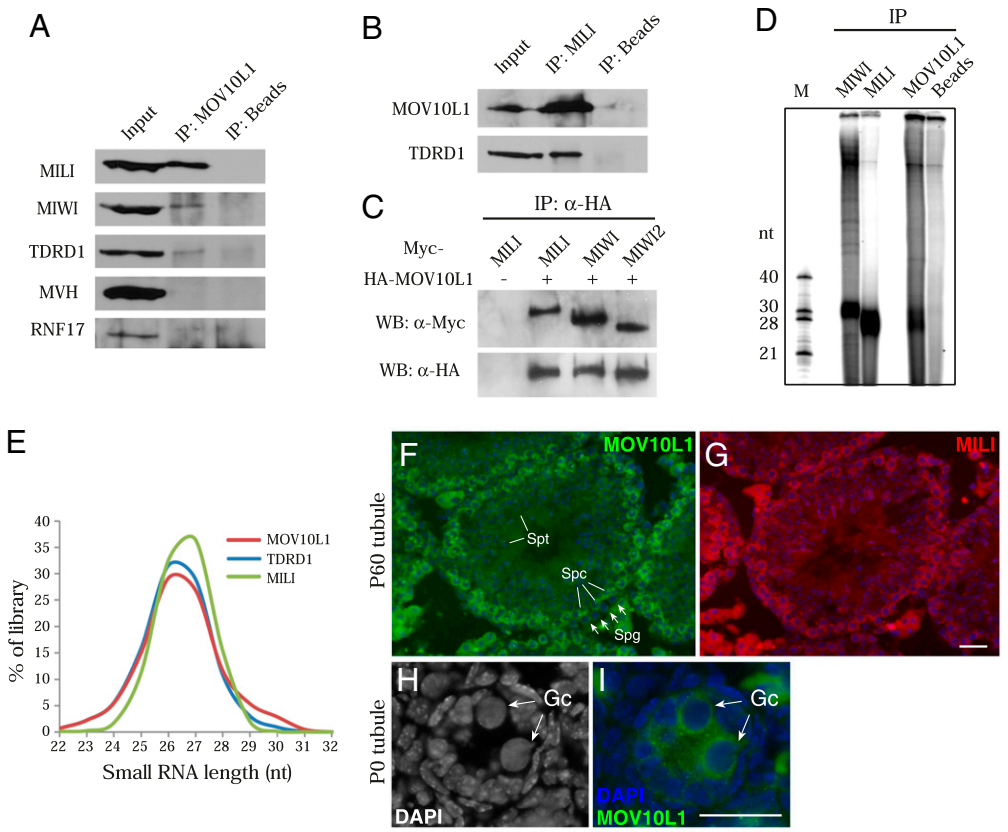

Fig. 1. MOV10L1 is associated with Piwi proteins and piRNAs in testis. (*A*) Validation of protein associations by coimmunoprecipitation (co-IP) and Western blotting. Note that nuage components MVH and RNF17 are not associated with MOV10L1. (*B*) Reciprocal IP confirms the association between MOV10L1 and MILI. (*C*) MOV10L1 interacts with MILI, MIWI, and MIWI2 in cotransfected 293T cells. (*D*) Analysis of piRNAs in immunoprecipitated MILI, MIWI, and MOV10L1 complexes from adult mouse testes. (*E*) Length distribution of small RNA reads in three small RNA libraries prepared from adult mouse testes. (*F* and *G*) Adjacent testis sections from 2-mo-old (P60) mice were immunostained with anti-MOV10L1 (*F*, green) and anti-MILI (*G*, red) antibodies. Strong interstitial signal is due to autofluorescence of Leydig cells. (*H* and *I*) Expression of MOV10L1 in gonocytes (Gc) from newborn (P0) testes. In contrast to nuclei of Sertoli cells, gonocyte nuclei contain little heterochromatin (*H*). Spg, spermatogonium; Spc, spermatocyte; Spt, spermatid. (Scale bar, 25 μm.)

library revealed that the majority of reads derive from intergenic (≈56%) unannotated regions, similar to MILI- and TDRD1-associated pachytene piRNAs from adult testes (Fig. S2*A*) (17, 20). Further analysis of the repeat fractions showed that representation of transposon classes is also similar among these three libraries (Fig. S2*B*). Pachytene piRNAs derive from ≈250 genomic regions, and this clustered origin is a hallmark of piRNA biogenesis. Reads from all three libraries mapped to the same strand within the same genomic window, confirming that the MOV10L1 reads are MILI-associated primary piRNAs (Fig. S2*C*). These results show that MOV10L1 is abundantly associated with the MILI–piRNA complex and, to a lesser extent, with the MIWI–piRNA complex in adult testis.

Colocalization of MOV10L1 with MILI in Male Germ Cells. We found that MOV10L1 localizes to the cytoplasm of germ cells. *Mov10l1* is transcribed at a much higher level in spermatocytes than in spermatogonia (21). Consistent with this previous study, the level of MOV10L1 protein in spermatogonia was low (Fig. 1*F*). MOV10L1 was clearly present in pachytene spermatocytes but absent in post-meiotic spermatids (Fig. 1*F*). This spatiotemporal localization pattern of MOV10L1 resembles that of MILI in adjacent testis sections (Fig. 1*G*). In postnatal day 14 (P14) tubules, MOV10L1 colocalized with GASZ, a nuage-associated protein in the piRNA pathway (22). Similar to MILI, MOV10L1 also localized to the cytoplasm of gonocytes from newborn testes (Fig. 1 *H* and *I*). These coexpression and colocalization data further support a role for MOV10L1 in the piRNA pathway.

MOV10L1 Is Essential for Male Meiosis and Male Fertility. To uncover the requirement of *Mov10l1* for spermatogenesis and the piRNA pathway, we generated a conditional mutant allele (*Mov10l1*^{fl}) in mice. In the targeted allele, one *loxP* site was inserted in intron 17 and one in intron 21 (Fig. S3). To disrupt the *Mov10l1* gene, *Mov10l1*^{fl} mice were bred with ACTB-Cre mice, in which Cre recombinase is ubiquitously expressed (23). Deletion of exons 18–21 (encoding amino acids 841–1,018) disrupted the putative RNA helicase domain of MOV10L1. Sequencing of the mutant *Mov10l1* transcript amplified from *Mov10l1*$^{-/-}$ testes showed that splicing occurred precisely from exon 17 to exon 22, maintaining the translation frame. As expected, the internally deleted MOV10L1 protein (1,061 aa; MOV10L1Δ) was expressed in *Mov10l1*$^{+/-}$ and *Mov10l1*$^{-/-}$ testes but with reduced abundance (Fig. 2*A*). The mutant MOV10L1 protein was not readily detectable in *Mov10l1*$^{-/-}$ testes by immunofluorescence (Fig. S4). Exons 17–27 of the *Mov10l1* locus are used to produce a heart-specific alternative transcript (termed *Csm*/*Champ*) (24, 25). Despite the lack of this heart-specific transcript, *Mov10l1*$^{-/-}$ mice were viable and exhibited no overt defects, suggesting that *Mov10l1* (*Csm*/*Champ*) is not essential for heart development. Interbreeding of heterozygous mice yielded a normal Mendelian ratio of offspring (*Mov10l1*$^{+/+}$, *Mov10l1*$^{+/-}$, *Mov10l1*$^{-/-}$: 56, 129, 63), suggesting that disruption of *Mov10l1* does not cause embryonic lethality.

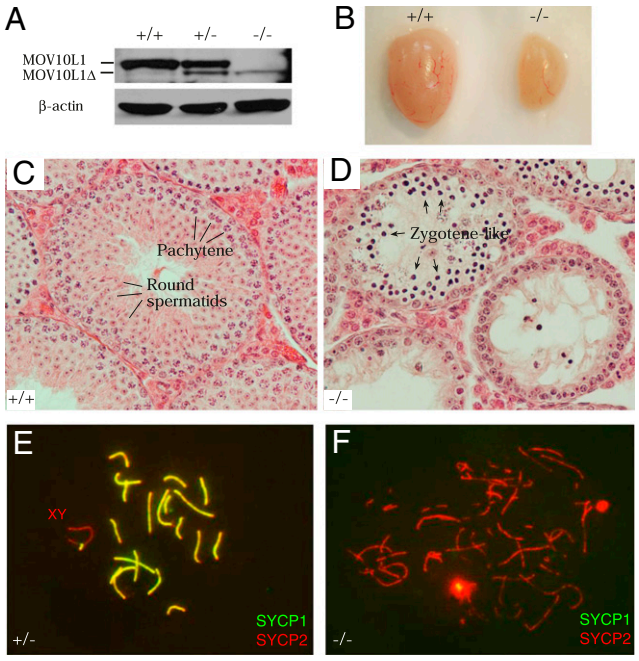

Fig. 2. *Mov10l1* is essential for spermatogenesis and chromosomal synapsis. (*A*) Western blot analysis of adult wild-type, *Mov10l1*$^{+/-}$, and *Mov10l1*$^{-/-}$ testes. The mutant MOV10L1 protein (1,061 aa; MOV10L1Δ) is indicated. (*B*) Dramatic size reduction in 7-wk-old *Mov10l1*$^{-/-}$ testis. (*C* and *D*) In contrast to wild-type tubules with full spermatogenesis (*C*), *Mov10l1*$^{-/-}$ tubules from adult mice exhibited early meiotic arrest (*D*). (*E*) Normal pachytene spermatocyte with 19 pairs of fully synapsed autosomes and the partially synapsed sex chromosomes. (*F*) Zygotene-like spermatocytes from *Mov10l1*$^{-/-}$ adult testes.

Mov10l1$^{-/-}$ females displayed normal fertility, but *Mov10l1*$^{-/-}$ males were sterile. Disruption of *Mov10l1* caused a sharp reduction in testis size (Fig. 2*B*). The weight of *Mov10l1*$^{-/-}$ testes (48.3 ± 9.1 mg per pair) from 5- to 7-wk-old mice was <37% that of *Mov10l1*$^{+/-}$ testes (131.1 ± 6.9 mg per pair) (Student's *t* test, $P < 0.0001$). In contrast to wild-type seminiferous tubules (Fig. 2*C*), tubules from adult *Mov10l1*$^{-/-}$ testes contained only early spermatogenic cells, with a complete lack of postmeiotic germ cells (Fig. 2*D*). The most advanced germ cells in the mutant were zygotene-like spermatocytes, indicating an early meiotic arrest. The stage of meiotic arrest in *Mov10l1*$^{-/-}$ mice is similar to that in *Mili* and *Miwi2* mutant mice (6, 26). Thus, MOV10L1 is required for male meiosis and is essential for male fertility.

To further define the meiotic defects in *Mov10l1*$^{-/-}$ testes, we analyzed the assembly of the synaptonemal complex by immunostaining central and axial elements with anti-SYCP1 and anti-SYCP2 antibodies. In *Mov10l1*$^{+/-}$ spermatocytes, all chromosomes were fully synapsed except the XY chromosomes, which were only synapsed at the pseudoautosomal region (Fig. 2*E*). In *Mov10l1*$^{-/-}$ spermatocytes, synapsis failed to occur, evident from the absence of SYCP1 (Fig. 2*F*). Thus, disruption of *Mov10l1* causes meiotic blockade before the pachytene stage.

MILI and TDRD1 Are Lost in *Mov10l1*$^{-/-}$ Spermatocytes but Retained in Spermatogonia. We next investigated the consequence of loss of MOV10L1 function on the expression of piRNA pathway components. Normally, MILI and TDRD1 are expressed in both spermatogonia and spermatocytes (Fig. S5). However, both MILI and TDRD1 were detectable in spermatogonia but not in spermatocytes in *Mov10l1*$^{-/-}$ testis (Fig. S5 *B* and *D*). In contrast, MVH, MAEL, and GASZ were still expressed in both spermatogonia and spermatocytes in *Mov10l1*$^{-/-}$ testis (Fig. S5*F*) (22, 27). The expression pattern of MILI and TDRD1 in P14 *Mov10l1*$^{-/-}$ testes was the same as in the adult (P60) mutant testes. Thus, disruption of MOV10L1 impacted the abundance of MILI and TDRD1 most dramatically. Decreased abundance of nuage proteins has also been observed in *Gasz* mouse mutant and a number of *Drosophila* nuage mutants (22, 28, 29).

Binary Derepression of LINE1 and IAP Retrotransposons in Postnatal *Mov10l1*$^{-/-}$ Testes. piRNAs are required for silencing of transposable elements in the germline in various species (1, 2, 30). We examined the expression of LINE1 and IAP retrotransposons in *Mov10l1*$^{-/-}$ testes. P10 testes contain predominantly spermatogonia and also preleptotene and leptotene spermatocytes. P14 testes also contain more advanced spermatocytes, such as zygotene and pachytene cells. Quantitative RT-PCR analyses showed that the abundance of both LINE1 and IAP transcripts increased sharply in *Mov10l1*$^{-/-}$ testes (Fig. 3*A*). We confirmed these findings by Northern blot analyses (Fig. 3*B*). Western blot analyses showed that LINE1 ORF1p abundance increased significantly in P10 *Mov10l1*$^{-/-}$ testes and more dramatically in P14 mutant testes (Fig. 3*C*). IAP protein abundance increased modestly in P10 and P14 *Mov10l1*$^{-/-}$ testes (Fig. 3*C*). Thus, disruption of *Mov10l1* results in derepression of LINE1 and IAP retrotransposons.

We next identified the cell types that express retrotransposon-encoded proteins by immunofluorescence analyses on adult testis sections (P60), in which spermatogonia and spermatocytes can be unequivocally identified. In wild-type tubules, LINE1 and IAP were barely detectable (Fig. 3*D*). *Mov10l1*$^{-/-}$ testes, however, exhibited highly abundant expression of LINE1 in spermatocytes but not spermatogonia (Fig. 3*E*). In contrast, IAP protein was readily visualized in spermatogonia but not in spermatocytes of mutant testes (Fig. 3*F*). This binary derepression pattern of LINE1 and IAP was also observed in P14 *Mov10l1*$^{-/-}$ testes. These data suggest that these two classes of retrotransposons (LINE1 and IAP) are silenced in a MOV10L1-dependent manner but are regulated differently in spermatogonia and spermatocytes.

Cytosine DNA methylation of retrotransposon regulatory regions in mouse causes transcriptional silencing (31). Methylation-sensitive Southern blotting showed that demethylation of LINE1 elements was discernible in *Mov10l1*$^{-/-}$ testes at P10 and clearly detectable in P14 mutant testes (Fig. 3*G*). Quantification of LINE1 demethylation by bisulfite sequencing showed methylation of 84% and 85% of CpGs in P10 and P14 *Mov10l1*$^{+/-}$ testes, respectively. Consistent with our Southern result, 72% of LINE1 CpGs were methylated in P10 *Mov10l1*$^{-/-}$ testes, but only 54% were methylated in P14 mutant testes. These data showed that disruption of *Mov10l1* results in loss of DNA methylation and thus derepression of LINE1 and IAP retrotransposons.

MILI Is Depleted of piRNAs in Postnatal *Mov10l1*$^{-/-}$ Testes. Given the association of MOV10L1 with the MILI piRNA ribonucleoprotein particles (piRNPs), we examined the impact of loss of *Mov10l1* on piRNA populations. In testes from P10 and P14 mice, MILI binds to prepachytene and pachytene piRNAs, respectively (8, 20). Although the abundance of MILI was reduced in *Mov10l1*$^{-/-}$ testes, a substantial amount of MILI was immunoprecipitated from P10 or P14 mutant testes but was found to be devoid of piRNAs in *Mov10l1*$^{-/-}$ testes (Fig. 4*A*). To rule out the possibility that the observed loss of MILI-bound piRNAs is due to the detection limit of immunoprecipitation and 5′-end radiolabeling assay, we repeated the experiment and, in parallel, performed immunoprecipitations with serial dilutions of P10 wild-type testis extract. MILI-associated piRNAs were readily detected in wild-type controls, even when MILI protein was not detectable by Western blotting (Fig. 4*B*, lanes 5 and 6), demonstrating the high sensitivity of this method. In conclusion, MILI is unloaded in the P10 and P14 *Mov10l1*$^{-/-}$ testes.

It is possible that, in *Mov10l1* mutant testes, piRNAs are produced but fail to get incorporated into MILI. To test this, we prepared and sequenced 18–32-nt total small RNA libraries from

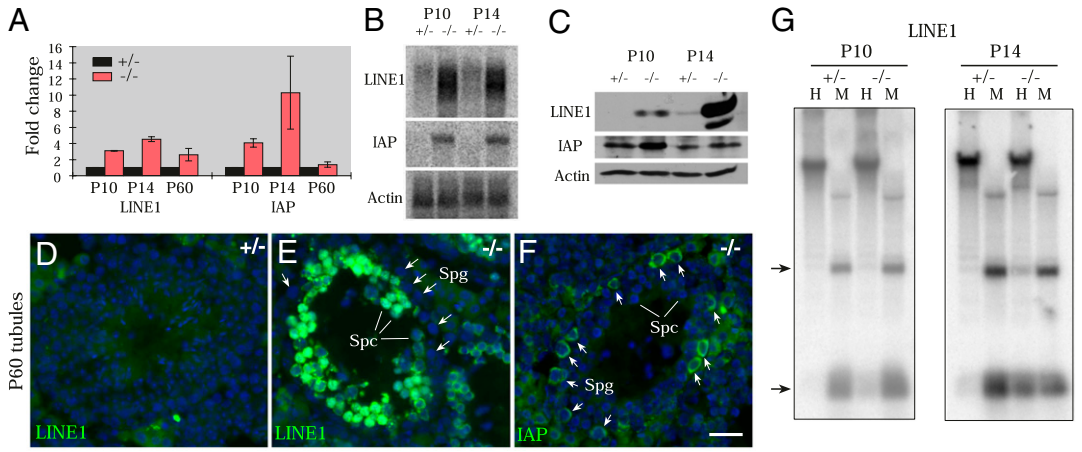

Fig. 3. Binary derepression of LINE1 and IAP retrotransposons in mitotic vs. meiotic germ cells. (*A*) Quantitative RT-PCR analysis. (*B*) Northern blot analysis. (*C*) Western blotting analysis. (*D* and *E*) Immuofluorescence analysis of LINE1 ORF1p in 2-mo-old (P60) *Mov10l1*$^{+/-}$ and *Mov10l1*$^{-/-}$ testes. (*F*) Immunofluorescence analysis of IAP in *Mov10l1*$^{-/-}$ testes. Spc, spermatocytes; Spg, spermatogonia. (*G*) Methylation-sensitive Southern blot analysis of testis genomic DNA. Genomic DNA was digested with methylation sensitive (HpaII, H) and methylation insensitive (MspI, M) enzymes. Arrows indicate the position of methylation-sensitive (H) restriction products in the *Mov10l1*$^{-/-}$ testes. (Scale bar in *F*, 25 μm for *D*–*F*.)

testes of P10 *Mov10l1*$^{+/-}$ and *Mov10l1*$^{-/-}$ mice. Analysis of read-lengths (Fig. 4*C*) revealed a loss of ≈26–28-nt sequences (presumably piRNAs) in *Mov10l1*$^{-/-}$ testes. The ≈21-nt reads, the bulk of which are annotated miRNAs, are still present in the *Mov10l1*$^{-/-}$ testes (Fig. 4*C*). These data demonstrate that MOV10L1 is required for biogenesis of piRNAs but not miRNAs.

Both MILI and MIWI2 Are Depleted of piRNAs in *Mov10l1*$^{-/-}$ Perinatal Germ Cells. Given that MOV10L1 is expressed in perinatal gonocytes (Fig. 1*I*), we wondered whether the piRNA pathway is affected in the early germ cells in *Mov10l1* mutant. We first examined the expression of MILI and MIWI2 in perinatal *Mov10l1*$^{-/-}$ germ cells. MIWI2 localized predominantly to the nucleus in P0 *Mov10l1*$^{+/-}$ gonocytes, but it was excluded from the nuclei and accumulated in the cytoplasm of *Mov10l1*$^{-/-}$ gonocytes (Fig. 4*D*). A nuclear-to-cytoplasmic redistribution of MIWI2 was also observed in both *Mili* and *Tdrd1* mouse mutants (5, 16, 17). The cytoplasmic localization of MILI was maintained in *Mov10l1*$^{-/-}$ gonocytes (Fig. 4*D*). Furthermore, LINE1 elements were strongly activated, and IAP was moderately derepressed in *Mov10l1*$^{-/-}$ gonocytes (Fig. S6). These data strongly indicate that the piRNA pathway is defective in *Mov10l1*$^{-/-}$ perinatal gonocytes.

In embryonic germ cells, MILI and MIWI2 are associated with repeat-rich prenatal piRNAs (5, 9). To ascertain the piRNA-association status of MILI and MIWI2 in *Mov10l1*$^{-/-}$ perinatal germ cells, we immunoprecipitated both proteins from P0 testes. In testes from *Mov10l1*$^{+/-}$ pups, MILI and MIWI2 were loaded with their respective ≈26- and ≈28-nt small RNAs. In contrast, both MILI and MIWI2 were completely devoid of piRNAs in *Mov10l1*$^{-/-}$ testes (Fig. 4*E*). Taken together with our findings in P10 and P14 mutant testes, we conclude that MOV10L1 is required for biogenesis and/or stability of both perinatal (MILI- or MIWI2-bound) and prepachytene (MILI-bound) piRNAs.

Discussion

Here we report a mouse mutant in which MILI-associated piRNAs are absent, whereas the MILI protein is still detectable. Our studies point to a central role for MOV10L1 in the biogenesis and/or stability of MILI-, MIWI2-, and possibly MIWI-bound piRNAs. First, we have demonstrated an essential role for MOV10L1 in the biogenesis of MILI-bound piRNAs in both perinatal (P0) and prepachytene (P10) stages. Second, MOV10L1 may also be directly required for the loading of presumably secondary piRNAs onto MIWI2 in perinatal gonocytes, because these two proteins bind to each other and MIWI2 is unloaded in the *Mov10l1* mutant. Alternatively, in the *Mov10l1* mutant, the "empty" MILI (lack of bound primary piRNAs) may fail to guide the biogenesis of secondary piRNAs that would bind to MIWI2. Such a possibility is further supported by the unloaded status of MIWI2 in the *Mili* mutant (5). Finally, the fact that MOV10L1 is associated with both MILI and MIWI in adult mouse testes also implicates it in the pachytene piRNA biogenesis. However, this is not readily testable, because disruption of *Mov10l1* causes meiotic block before the pachytene stage.

MOV10L1 exhibits limited homology with MOV10, which is the vertebrate homolog of *Drosophila* Armi. Armi is a sequence homolog of SDE3, which is required for posttranscriptional gene silencing in *Arabidopsis* (32). Armi is required for RISC maturation and *oskar* mRNA silencing (33, 34). Armi is also important for piRNA biogenesis and silencing of the *Stellate* repeat locus and retrotransposons (28, 35). Therefore, Armi functions in both RNAi and piRNA pathways in *Drosophila*. Our data demonstrate that the vertebrate-specific MOV10L1 is specialized in the piRNA pathway.

Members of the RNA helicase superfamily are required for all biological processes involving RNA molecules, such as ribosome biogenesis, splicing, translation, and RNA interference (36). MOV10L1 is a putative RNA helicase that contains all of the conserved helicase motifs, including ATPase and unwindase domains. Our findings that the truncated mutant protein lacks only the RNA helicase domain and is defective in piRNA biogenesis demonstrate that this domain is required for MOV10L1 functions. Biochemical studies of *Drosophila* Armi suggest that Armi facilitates ATP-dependent incorporation of single-stranded siRNA into RISC (34). Analogous to the role of Armi in RISC maturation, MOV10L1 may facilitate loading of piRNAs into piRNP complexes. One explanation for the loss of 25–32-nt small RNAs (piRNAs) in the total small RNA library from P10 *Mov10l1* mutant testes is that piRNAs are generated but fail to incorporate into MILI and thus are degraded. Alternatively, MOV10L1 might be required for the primary processing in the biogenesis of piRNAs.

Materials and Methods

Antibodies, Western Blot Analyses, and DNA Constructs. Two GST-MOV10L1 (amino acids 1–101 and 53–253) fusion proteins were expressed in *Escherichia coli*. Purified recombinant proteins were used to immunize rabbits. Other antibodies used were MILI (Abcam), MIWI (Abcam), MIWI2 (J. Martinez and G. Hannon), TDRD1, RNF17, MVH (T. Noce), LINE1 ORF1p (S. L. Martin), IAP

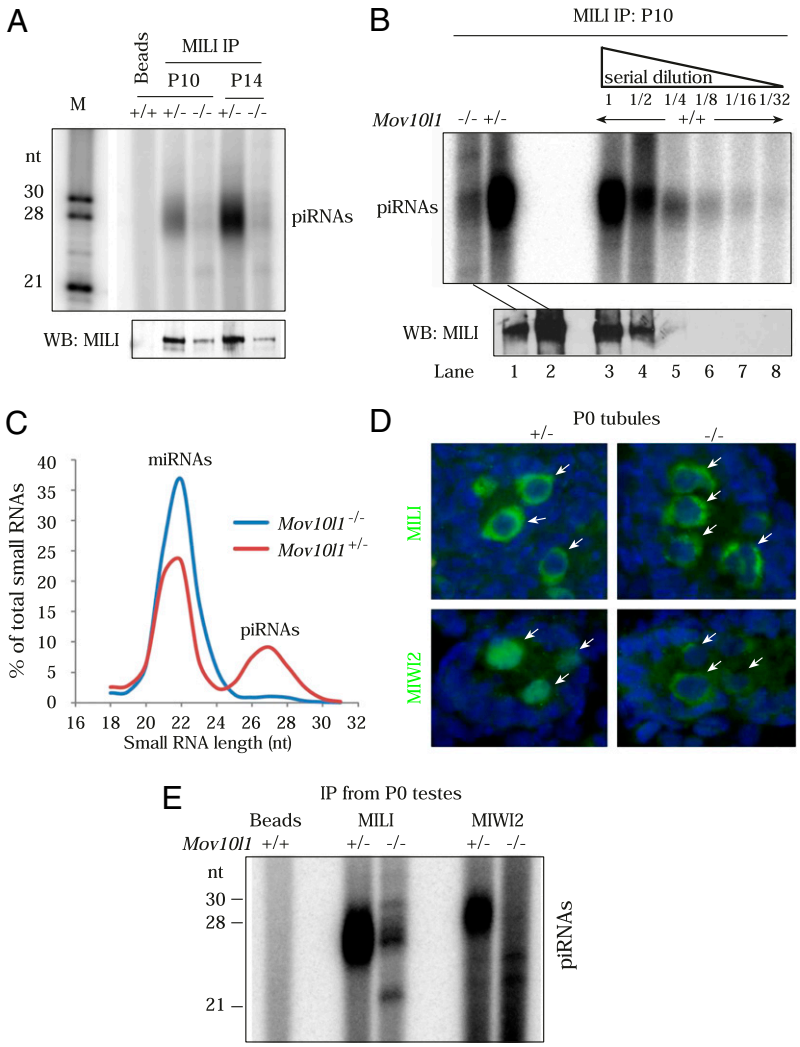

Fig. 4. Biogenesis blockade of both prepachytene and perinatal piRNAs in *Mov10l1*$^{-/-}$ testes. (*A*) MILI is unloaded in P10 and P14 *Mov10l1*$^{-/-}$ testes. One tenth of the immunoprecipitated material was used for detection of associated RNAs, whereas the remaining was used for Western blotting (WB) to detect MILI. (*B*) MILI immunoprecipitations with P10 *Mov10l1*$^{-/-}$, *Mov10l1*$^{+/-}$, and serial dilutions (1:2) of P10 wild-type testicular extracts. (*C*) Profile of read lengths in total small RNA (18–32 nt) libraries from P10 *Mov10l1*$^{+/-}$ and *Mov10l1*$^{-/-}$ testes. (*D*) MIWI2 is localized to the cytoplasm in *Mov10l1*$^{-/-}$ perinatal (P0) gonocytes (arrows). (*E*) MILI and MIWI2 are devoid of piRNAs in *Mov10l1*$^{-/-}$ newborn (P0) testes.

GAG (B. R. Cullen), MAEL (Abcam), GASZ (M. M. Matzuk), β-actin (Sigma-Aldrich), HA (Santa Cruz Biotechnology), and Myc (EMBL MACF).

Coding sequences for *Miwi*, *Miwi2*, and *Mili* were cloned into the pcDNA3 vector with an N-terminal 3× Myc tag. The *Mov10l1* ORF was inserted into the pCIneo vector with an N-terminal HA tag. Plasmids were cotransfected into HEK 293T cells, and lysates were prepared after 48 h for immunoprecipitations.

Immunoprecipitation, Mass Spectrometry, and Detection of Small RNAs. Eight pairs of 18- to 20-d testes (≈300 mg) were used for immunoprecipitation with affinity-purified anti-MOV10L1 antibody followed by SDS/PAGE. Gel bands of interest were cut and sent for protein identification by mass spectrometry at the PENN Proteomics Core facility.

Mouse testicular extract preparation, immunoprecipitations, purification of MILI complexes for complex identification, and 5′ end-labeling of piRNAs were performed as described previously (17). Equal numbers of age-matched *Mov10l1*$^{+/-}$ or *Mov10l1*$^{-/-}$ testes were used in experiments describing small RNA association with MILI and MIWI2 (Fig. 4).

Targeted Inactivation of the *Mov10l1* Gene. To generate the *Mov10l1* targeting construct, DNA fragments were amplified by high-fidelity PCR using a *Mov10l1* BAC clone (RP23-269F24) as template. V6.5 ES cells were electroporated with linearized *Mov10l1* targeting construct (pKe16-1/ClaI). Screening of ES cells was described previously (37). Two ES cell clones (A1 and B10) harboring the *Mov10l1*^{fl} allele were injected into B6C3F1 (Taconic) blastocysts. The *Mov10l1*^{fl} allele was transmitted through the germline in chimeric mice derived from both clones. All offspring were genotyped by PCR. Wild-type (398 bp) and floxed (592 bp) alleles were assayed by PCR with the primers GGCCTATGGGTTGAATGTGT and CAGGAAGAGCAGGTGAAGTG. The *Mov10l1* knockout (461 bp) allele was assayed by PCR with the primers GGGTCGTGGATCTGGGATAT and CAGGAAGAGCAGGTGAAGTG.

Histological, Surface-Spread, and Immunofluorescence Analyses. For histology, testes were fixed in Bouin's solution overnight, dehydrated in ethanol, embedded in paraffin, sectioned, and stained with hematoxylin and eosin. Surface-spread analysis of spermatocyte nuclei and immunofluorescence analyses of testis sections were described previously (37).

Southern and Northern Blot Analyses. Methylation-sensitive Southern blot, Northern blot, and bisulfite analyses were described previously (17).

Small RNA Library Construction, Sequencing, and Bioinformatic Analyses. MOV10L1-associated small RNAs from adult mouse testes extract and 18–32-nt total small RNAs from *Mov10l1*$^{+/-}$ and *Mov10l1*$^{-/-}$ P10 testes were used for preparation of libraries for deep sequencing by Solexa technology (Illumina). MILI and TDRD1 libraries were previously described (17). Sequencing reads that perfectly mapped to the mouse genome were considered for

analyses: MOV10L1 (≈2.2 million), *Mov10l1*$^{-/-}$ (≈500,000), and *Mov10l1*$^{+/-}$ (≈125,000). Small RNA sequencing data used in this study are deposited in the GEO database under the accession number GSE21763.

ACKNOWLEDGMENTS. We thank the following for gifts of antibodies: J. Martinez (Institute of Molecular Biotechnology GmbH, Vienna) and G. Hannon (Cold Spring Harbor Laboratory, Cold Spring Harbor, NY) for MIWI2 antibody, B. R. Cullen (Duke University Medical Center, Durham, NC) for IAP antibody, S. L. Martin (University of Colorado School of Medicine, Denver) for L1 ORF1p antibody, M. M. Matzuk (Baylor College of Medicine, Houston) for GASZ antibody, T. Noce (Shiga University of Medical Science, Shiga, Japan) for MVH antibody, and C. Höög (Karolinska Institutet, Stockholm) for SYCP1 antibody; we also thank C. Yuan for mass spectrometry and Stephanie Eckhardt for imaging analysis; the European Molecular Biology Laboratory (EMBL) Protein Expression and Gene Core facilities for antibody production and Solexa sequencing; and D. O'Carroll, F. Yang, A. Verdel, and members of the Pillai group for comments on the manuscript. This work was supported by EMBL (R.S.P.), Agence National de la Recherche Jeune Chercheur program (piRmachines) (R.S.P), and National Institutes of Health/National Institute of General Medical Sciences Grant RO1GM076327 (to P.J.W.).

1. Ghildiyal M, Zamore PD (2009) Small silencing RNAs: An expanding universe. *Nat Rev Genet* 10:94–108.
2. Malone CD, Hannon GJ (2009) Small RNAs as guardians of the genome. *Cell* 136: 656–668.
3. Kim VN, Han J, Siomi MC (2009) Biogenesis of small RNAs in animals. *Nat Rev Mol Cell Biol* 10:126–139.
4. Thomson T, Lin H (2009) The biogenesis and function of PIWI proteins and piRNAs: Progress and prospect. *Annu Rev Cell Dev Biol* 25:355–376.
5. Aravin AA, et al. (2008) A piRNA pathway primed by individual transposons is linked to de novo DNA methylation in mice. *Mol Cell* 31:785–799.
6. Kuramochi-Miyagawa S, et al. (2004) Mili, a mammalian member of piwi family gene, is essential for spermatogenesis. *Development* 131:839–849.
7. Deng W, Lin H (2002) miwi, a murine homolog of piwi, encodes a cytoplasmic protein essential for spermatogenesis. *Dev Cell* 2:819–830.
8. Aravin AA, Sachidanandam R, Girard A, Fejes-Toth K, Hannon GJ (2007) Developmentally regulated piRNA clusters implicate MILI in transposon control. *Science* 316:744–747.
9. Kuramochi-Miyagawa S, et al. (2008) DNA methylation of retrotransposon genes is regulated by Piwi family members MILI and MIWI2 in murine fetal testes. *Genes Dev* 22:908–917.
10. Gunawardane LS, et al. (2007) A slicer-mediated mechanism for repeat-associated siRNA 5′ end formation in *Drosophila*. *Science* 315:1587–1590.
11. Brennecke J, et al. (2007) Discrete small RNA-generating loci as master regulators of transposon activity in *Drosophila*. *Cell* 128:1089–1103.
12. Wang PJ, McCarrey JR, Yang F, Page DC (2001) An abundance of X-linked genes expressed in spermatogonia. *Nat Genet* 27:422–426.
13. Meister G, et al. (2005) Identification of novel argonaute-associated proteins. *Curr Biol* 15:2149–2155.
14. Chendrimada TP, et al. (2007) MicroRNA silencing through RISC recruitment of eIF6. *Nature* 447:823–828.
15. Chen C, et al. (2009) Mouse piwi interactome identifies binding mechanism of tdrkh tudor domain to arginine methylated miwi. *Proc Natl Acad Sci USA* 106:20336–20341.
16. Vagin VV, et al. (2009) Proteomic analysis of murine Piwi proteins reveals a role for arginine methylation in specifying interaction with Tudor family members. *Genes Dev* 23:1749–1762.
17. Reuter M, et al. (2009) Loss of the Mili-interacting Tudor domain-containing protein-1 activates transposons and alters the Mili-associated small RNA profile. *Nat Struct Mol Biol* 16:639–646.
18. Girard A, Sachidanandam R, Hannon GJ, Carmell MA (2006) A germline-specific class of small RNAs binds mammalian Piwi proteins. *Nature* 442:199–202.
19. Grivna ST, Beyret E, Wang Z, Lin H (2006) A novel class of small RNAs in mouse spermatogenic cells. *Genes Dev* 20:1709–1714.
20. Aravin A, et al. (2006) A novel class of small RNAs bind to MILI protein in mouse testes. *Nature* 442:203–207.
21. Wang PJ, Page DC, McCarrey JR (2005) Differential expression of sex-linked and autosomal germ-cell-specific genes during spermatogenesis in the mouse. *Hum Mol Genet* 14:2911–2918.
22. Ma L, et al. (2009) GASZ is essential for male meiosis and suppression of retrotransposon expression in the male germline. *PLoS Genet* 5:e1000635.
23. Lewandoski M, Meyers EN, Martin GR (1997) Analysis of Fgf8 gene function in vertebrate development. *Cold Spring Harb Symp Quant Biol* 62:159–168.
24. Ueyama T, Kasahara H, Ishiwata T, Yamasaki N, Izumo S (2003) Csm, a cardiac-specific isoform of the RNA helicase Mov10l1, is regulated by Nkx2.5 in embryonic heart. *J Biol Chem* 278:28750–28757.
25. Liu ZP, Olson EN (2002) Suppression of proliferation and cardiomyocyte hypertrophy by CHAMP, a cardiac-specific RNA helicase. *Proc Natl Acad Sci USA* 99:2043–2048.
26. Carmell MA, et al. (2007) MIWI2 is essential for spermatogenesis and repression of transposons in the mouse male germline. *Dev Cell* 12:503–514.
27. Soper SF, et al. (2008) Mouse maelstrom, a component of nuage, is essential for spermatogenesis and transposon repression in meiosis. *Dev Cell* 15:285–297.
28. Malone CD, et al. (2009) Specialized piRNA pathways act in germline and somatic tissues of the Drosophila ovary. *Cell* 137:522–535.
29. Li C, et al. (2009) Collapse of germline piRNAs in the absence of Argonaute3 reveals somatic piRNAs in flies. *Cell* 137:509–521.
30. Aravin AA, Hannon GJ, Brennecke J (2007) The Piwi-piRNA pathway provides an adaptive defense in the transposon arms race. *Science* 318:761–764.
31. Bourc'his D, Bestor TH (2004) Meiotic catastrophe and retrotransposon reactivation in male germ cells lacking Dnmt3L. *Nature* 431:96–99.
32. Dalmay T, Horsefield R, Braunstein TH, Baulcombe DC (2001) SDE3 encodes an RNA helicase required for post-transcriptional gene silencing in Arabidopsis. *EMBO J* 20: 2069–2078.
33. Cook HA, Koppetsch BS, Wu J, Theurkauf WE (2004) The *Drosophila* SDE3 homolog armitage is required for oskar mRNA silencing and embryonic axis specification. *Cell* 116:817–829.
34. Tomari Y, et al. (2004) RISC assembly defects in the *Drosophila* RNAi mutant armitage. *Cell* 116:831–841.
35. Vagin VV, et al. (2006) A distinct small RNA pathway silences selfish genetic elements in the germline. *Science* 313:320–324.
36. Tanner NK, Linder P (2001) DExD/H box RNA helicases: From generic motors to specific dissociation functions. *Mol Cell* 8:251–262.
37. Yang F, et al. (2008) Meiotic failure in male mice lacking an X-linked factor. *Genes Dev* 22:682–691.